

## Magnetic properties of $R_2\text{Mn}_2\text{O}_7$ pyrochlore rare-earth solid solutions

N. Imamura,<sup>1</sup> M. Karppinen,<sup>1,2,\*</sup> H. Yamauchi,<sup>1,2</sup> and J. B. Goodenough<sup>3</sup>

<sup>1</sup>Materials and Structures Laboratory, Tokyo Institute of Technology, Yokohama 226-8503, Japan

<sup>2</sup>Laboratory of Inorganic Chemistry, Department of Chemistry, Aalto University, FI-00076 AALTO, Finland

<sup>3</sup>Texas Materials Institute, The University of Texas at Austin, Austin, Texas 78712, USA

(Received 13 July 2010; published 28 October 2010)

Three  $(R,R')_2\text{Mn}_2\text{O}_7$  ferromagnetic pyrochlore systems were studied to investigate the role of the  $R^{3+}$  ionic size versus  $4f$  moment on the magnetic properties of the  $\text{Mn}_2\text{O}_7$  sublattice. The Curie temperature  $T_C = 18 \pm 1$  K for  $R=\text{Y}$  and  $\text{Lu}$  remained nearly constant for  $(\text{Y}_{1-x}\text{Lu}_x)_2\text{Mn}_2\text{O}_7$  but the magnetization data show characteristics of spin-glass behavior in low magnetic fields, and at 5 T, the magnetization fails to reach the expected  $3 \mu_B/\text{Mn}^{4+}$  found by 0.5 T in  $\text{Tl}_2\text{Mn}_2\text{O}_7$  and  $\text{In}_2\text{Mn}_2\text{O}_7$ . A frustrated, minor antiferromagnetic component apparently competes with the ferromagnetic component of the  $\text{Mn}^{4+}\text{-O-Mn}^{4+}$  interactions to give a minor antiferromagnetic component to the major ferromagnetic spin alignment of the  $\text{Mn}^{4+}$  ions. A  $T_C = 42 \pm 1$  K for  $R=\text{Dy}$  and  $\text{Yb}$  remains nearly constant in the  $(\text{Dy}_{1-y}\text{Yb}_y)_2\text{Mn}_2\text{O}_7$  system and  $T_C$  increases systematically from 19 to 42 K with Dy concentration in  $(\text{Dy}_{1-z}\text{Lu}_z)_2\text{Mn}_2\text{O}_7$ , which clearly shows that a ferromagnetic interaction between the  $R^{3+}$ -ion and  $\text{Mn}^{4+}$ -ion spins favors ferromagnetic alignment of the  $\text{Mn}^{4+}$ -ion spins to double the magnitude of  $T_C$  by relieving the frustration of the  $\text{Mn}_2\text{O}_7$  sublattice. The  $R^{3+}$ -ion size has little effect as the Mn-O-Mn bond angle changes by no more than  $\sim 1^\circ$  with changing ionic radius of the  $R^{3+}$  ion.

DOI: 10.1103/PhysRevB.82.132407

PACS number(s): 75.47.Lx, 75.50.Dd

### I. INTRODUCTION

Crystals containing geometrically frustrated interacting spins have attracted much attention for their variety of exciting physical properties stemming from the competing interactions that prevent the spin system from an ordering that optimizes every interaction. Pyrochlore oxides with the general formula  $A_2B_2O_7$  ( $A$ =trivalent cation;  $B$ =tetraivalent cation) form one of the well-known examples of such crystals.<sup>1</sup> In the cubic pyrochlore structure, the two cation species,  $A$  and  $B$ , are independently arranged into corner-sharing cation tetrahedra forming three-dimensional mutually interpenetrating sublattices. Oxygen atoms are then situated in such a way that each  $A$  cation is surrounded by eight oxygen atoms and each  $B$  cation by six oxygen atoms. Interesting magnetic and transport properties such as spin-glass (SG),<sup>2,3</sup> spin-ice<sup>4-6</sup> and spin-liquid<sup>7</sup> states, colossal magnetoresistivity,<sup>8,9</sup> an anomalous Hall effect,<sup>10</sup> a metal-insulator transition,<sup>2</sup> and superconductivity<sup>11</sup> have been revealed for the pyrochlore oxides.

The Mn-based pyrochlore oxides,  $A_2\text{Mn}_2\text{O}_7$ , can be prepared through high-pressure (HP) synthesis for small rare-earth elements ( $R=\text{Sc}$ ,  $\text{Y}$ ,  $\text{Dy-Lu}$ ) (Refs. 12 and 13) and also for  $\text{In}$  and  $\text{Tl}$  (Refs. 8, 9, and 14) as the  $A$  constituent. The pyrochlore  $\text{Tl}_2\text{Mn}_2\text{O}_7$  is metallic, whereas  $\text{In}_2\text{Mn}_2\text{O}_7$  and  $R_2\text{Mn}_2\text{O}_7$  are semiconducting. All the  $A_2\text{Mn}_2\text{O}_7$  phases are ferromagnetic (FM) at low temperatures, the fact being well explained by a dominant FM Mn-O-Mn superexchange interaction for the peculiar Mn-O-Mn bond angle of about  $130^\circ$ .<sup>14</sup> According to the Goodenough-Kanamori rules,<sup>15,16</sup> an antiferromagnetic (AFM)  $180^\circ$  Mn-O-Mn superexchange interaction changes to an FM interaction as the Mn-O-Mn bond angle decreases to less than about  $135^\circ$ . However, an AFM Mn-Mn superexchange is also present at smaller bond angles and it dominates the  $90^\circ$  Mn-O-Mn interaction where the  $\text{Mn}^{4+}$  octahedra share common edges in an oxide. With a  $130^\circ$  Mn-O-Mn bond angle, the larger Mn-Mn separation

makes dominant the FM Mn-O-Mn interactions, but it is clear that the strength of a net FM interaction between octahedral-site  $\text{Mn}^{4+}$  ions depends sensitively on the Mn-O-Mn bond angle. The bond angle changes progressively with  $R^{3+}$ -ion size in the  $\text{RMO}_3$  perovskites but the bond angle is not sensitive to the  $R^{3+}$ -ion size in the  $R_2\text{Mn}_2\text{O}_7$  pyrochlore structure.<sup>12,14</sup> The FM transition temperature  $T_C$  is much higher for  $\text{Tl}_2\text{Mn}_2\text{O}_7$  and  $\text{In}_2\text{Mn}_2\text{O}_7$  (over 120 K) than for  $\text{Lu}_2\text{Mn}_2\text{O}_7$  and  $\text{Y}_2\text{Mn}_2\text{O}_7$  (below 20 K), which may be attributed to strong hybridization of  $\text{In}(5s)/\text{Tl}(6s)$  orbitals with  $\text{O}(2p)$  and  $\text{Mn}(3d)$  orbitals enhancing the FM interaction (and simultaneously the electrical conductivity).<sup>14</sup> Within the  $R_2\text{Mn}_2\text{O}_7$  system, however, the  $T_C$  value deviates from any systematic trend expected on the basis of the  $R^{3+}$  constituent size, which implies that a magnetic  $R^{3+}$  constituent (or  $4f$  moment) may give an additional contribution to the magnetic behavior.<sup>12,14,17-19</sup> Apparently the  $R_2\text{Mn}_2\text{O}_7$  system differs in the nature of its magnetic phase transition from other pyrochlore oxide systems such as  $R_2\text{Mo}_2\text{O}_7$  (Ref. 20) and  $R_2\text{Ru}_2\text{O}_7$ .<sup>21-23</sup> So far based on several complementary experimental techniques, it has been revealed that the magnetism of  $R_2\text{Mn}_2\text{O}_7$  is of the reentrant-SG (RSG) type at low temperatures.<sup>17,18</sup>

A so-called magnetic dilution realized, for instance, by gradually substituting nonmagnetic  $R^{3+}$  ions for magnetic  $R^{3+}$  ions<sup>5,24,25</sup> is a highly useful approach to deepen our understanding of complex magnetic systems, including the present  $R_2\text{Mn}_2\text{O}_7$  system. However, as different  $R$  constituents in general are of different sizes, such a substitution inevitably involves some local structural changes that may affect the nature of the superexchange interactions. For example, the  $R_2\text{Mo}_2\text{O}_7$  system was extensively studied and shown to exhibit a universal dependence of  $T_C$  on the mean ionic radius of the constituent  $R^{3+}$  ions,  $r(R^{3+})$ .<sup>2,26-28</sup> In the present study we investigate three different pyrochlore manganese-oxide solid-solution systems, (i)  $(\text{Y}_{1-x}\text{Lu}_x)_2\text{Mn}_2\text{O}_7$ , (ii)  $(\text{Dy}_{1-y}\text{Yb}_y)_2\text{Mn}_2\text{O}_7$ , and (iii)

$(\text{Dy}_{1-z}\text{Lu}_z)_2\text{Mn}_2\text{O}_7$ . In all the three systems (i)–(iii) the lattice shrinks with increasing substitution level, i.e., with increasing  $x$ ,  $y$ , or  $z$ , suggesting a systematic increase in the degree of chemical pressure on the  $\text{Mn}_2\text{O}_7$  array. The (i) “nonmagnetic- $R$ ” system,  $(\text{Y,Lu})_2\text{Mn}_2\text{O}_7$ , contains only nonmagnetic  $R^{3+}$  ions whereas in the other two systems, (ii) and (iii), the host  $R^{3+}$  cation ( $=\text{Dy}^{3+}$ ) is magnetic. In the (ii) “magnetic-moment-diluted”  $(\text{Dy,Yb})_2\text{Mn}_2\text{O}_7$  system, not only the host but also the substituent is magnetic, but with a smaller magnetic moment compared to that of the host. In the (iii) “magnetic-ion-diluted”  $(\text{Dy,Lu})_2\text{Mn}_2\text{O}_7$  system, the substituent is nonmagnetic. Additionally we synthesize and characterize another type of magnetic-ion-diluted sample,  $(\text{Dy}_{0.5}\text{Y}_{0.5})_2\text{Mn}_2\text{O}_7$ , in which the two  $R^{3+}$  cation constituents are of nearly equal size.

## II. EXPERIMENTAL

Essentially single-phase samples of  $(\text{Y}_{1-x}\text{Lu}_x)_2\text{Mn}_2\text{O}_7$  ( $x = 0.3, 0.5, 0.8$ , and  $1.0$ ),  $(\text{Dy}_{1-y}\text{Yb}_y)_2\text{Mn}_2\text{O}_7$  ( $y = 0.0, 0.3, 0.5, 0.8$ , and  $1.0$ ),  $(\text{Dy}_{1-z}\text{Lu}_z)_2\text{Mn}_2\text{O}_7$  ( $z = 0.0, 0.2, 0.5, 0.7, 0.9$ , and  $1.0$ ), and  $(\text{Dy}_{0.5}\text{Y}_{0.5})_2\text{Mn}_2\text{O}_7$  were synthesized by means of an HP technique from stoichiometric ratios (in terms of cation stoichiometry) of  $R_2\text{O}_3$  and  $\text{Mn}_2\text{O}_3/\text{MnCO}_3$ . Prior to HP syntheses, raw-material powder mixtures were calcined in air at  $1300^\circ\text{C}$  for 24 h. The excess oxygen required for stabilizing the Mn-based pyrochlore phases was provided from  $\text{KClO}_3$  which was mixed with the precursor powder before loading the calcined powder in a gold capsule. High-pressure syntheses were then carried out with a cubic-anvil-type HP apparatus at 5 GPa and  $1000^\circ\text{C}$  for 30 min. From the HP product, residual KCl was washed out with distilled water. All the samples were then characterized for phase purity by x-ray powder diffraction (XRD; Rigaku: RINT2550VK/U equipped with a rotating Cu anode; Cu  $K\alpha$  radiation). The diffraction patterns were readily indexed with cubic space group  $Fd\bar{3}m$  expected for the Mn-based pyrochlore oxides.<sup>12,19</sup> The lattice parameter  $a$  was determined from the XRD data with the software JANA2000 (Ref. 29) in the profile-fitting mode. The dc magnetization ( $M$ ) was measured for the samples in a temperature range of 5–400 K in both zero-field-cooled (ZFC) and field-cooled (FC) modes with a superconducting quantum interference device magnetometer (Quantum Design: MPMS-XL5).

## III. RESULTS AND DISCUSSION

Judging from the XRD patterns (not presented here), all the samples were essentially single phase. The lattice parameters  $a$  calculated from the XRD data are plotted in Figs. 1(a)–1(c) for the three sample series, (i)  $(\text{Y}_{1-x}\text{Lu}_x)_2\text{Mn}_2\text{O}_7$ , (ii)  $(\text{Dy}_{1-y}\text{Yb}_y)_2\text{Mn}_2\text{O}_7$ , and (iii)  $(\text{Dy}_{1-z}\text{Lu}_z)_2\text{Mn}_2\text{O}_7$ , against the tabulated average ionic radius,  $r(R^{3+})$  for eightfold coordination.<sup>30</sup> For the end members, i.e.,  $R_2\text{Mn}_2\text{O}_7$  with single  $R$  constituents, the  $a$  values are in good agreement with those previously reported.<sup>12–14,19</sup> For solid-solution compositions, the  $a$  value depends linearly on the average ionic radius  $r(R^{3+})$ . Therefore we may conclude that the mean Mn-O bond length systematically decreases with de-

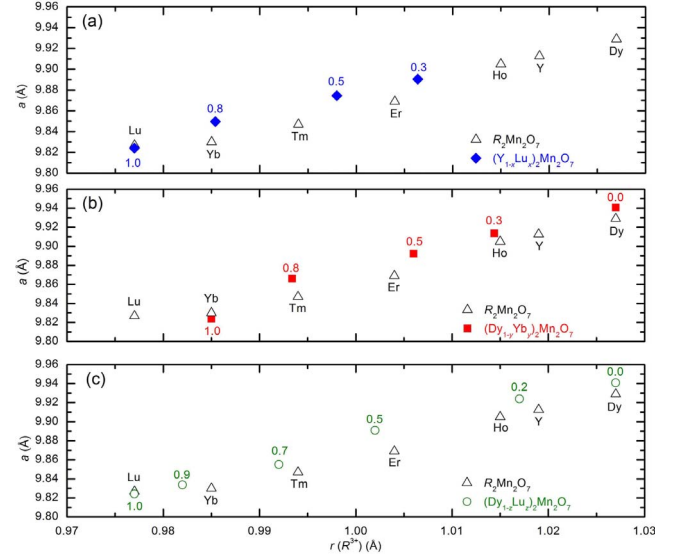


FIG. 1. (Color online) Lattice parameter  $a$  plotted as a function of the average ionic radius of the  $R$  cation(s),  $r(R^{3+})$ , for (a)  $(\text{Y}_{1-x}\text{Lu}_x)_2\text{Mn}_2\text{O}_7$ , (b)  $(\text{Dy}_{1-y}\text{Yb}_y)_2\text{Mn}_2\text{O}_7$ , and (c)  $(\text{Dy}_{1-z}\text{Lu}_z)_2\text{Mn}_2\text{O}_7$ . Data for the  $R_2\text{Mn}_2\text{O}_7$  phases ( $\Delta$ ; taken from Ref. 31) are given for comparison.

creasing  $r(R^{3+})$ ; however, the Mn-O-Mn bond angle changes by no more than  $\sim 1^\circ$ .<sup>12,14</sup>

The magnetic susceptibility ( $\chi$ ) versus temperature ( $T$ ) curves for the (i) nonmagnetic  $R$   $(\text{Y}_{1-x}\text{Lu}_x)_2\text{Mn}_2\text{O}_7$  system are presented in Fig. 2(a). All the samples show an FM transition around  $T_C = 17 \pm 1$  K; accordingly it is clear that  $T_C$  does not depend significantly on  $r(R^{3+})$ . Magnetization data for the (ii) magnetic-moment-diluted  $(\text{Dy}_{1-y}\text{Yb}_y)_2\text{Mn}_2\text{O}_7$  and (iii) magnetic-ion-diluted  $(\text{Dy}_{1-z}\text{Lu}_z)_2\text{Mn}_2\text{O}_7$  systems are shown in Figs. 2(b) and 2(c), respectively. All the  $(\text{Dy}_{1-y}\text{Yb}_y)_2\text{Mn}_2\text{O}_7$  samples show an FM transition at  $T_C = 42 \pm 1$  K, whereas for the  $(\text{Dy}_{1-z}\text{Lu}_z)_2\text{Mn}_2\text{O}_7$  samples  $T_C$  decreases from 42 K (for  $z = 0.0$ ) to 19 K (for  $z = 1.0$ ). Here we should mention that for the *ad hoc*  $(\text{Dy}_{0.5}\text{Y}_{0.5})_2\text{Mn}_2\text{O}_7$  sample, the  $T_C$  value was determined at 35 K (not shown in Fig. 2), which is close to the value (39 K) observed for  $(\text{Dy}_{0.5}\text{Lu}_{0.5})_2\text{Mn}_2\text{O}_7$ . To visualize the above findings, we plot  $T_C$  against  $r(R^{3+})$  in Fig. 3 for all the samples (i)–(iii) and also include, for comparison, the  $T_C$  values of nondoped  $R_2\text{Mn}_2\text{O}_7$  phases with single  $R$  constituents as given in Ref. 31. From Fig. 3 it is clearly revealed that the  $T_C$  value does not depend simply on  $r(R^{3+})$  but increases with increasing additional concentration of magnetic  $R^{3+}$  ions. It moreover seems that the primary factor is not the average magnetic moment [cf. the essentially constant  $T_C$  for the magnetic-moment-diluted  $(\text{Dy}_{1-y}\text{Yb}_y)_2\text{Mn}_2\text{O}_7$  system] but the concentration of magnetic ions in the rare-earth sublattice [cf. the decreasing  $T_C$  in the magnetic-ion-diluted  $(\text{Dy}_{1-z}\text{Lu}_z)_2\text{Mn}_2\text{O}_7$  system with  $z$ ].

We also observe from Figs. 2(a)–2(c) that, in contrast to the  $(\text{Y,Lu})_2\text{Mn}_2\text{O}_7$  system, a clear branching of the magnetization curve between ZFC and FC modes is observed for both the  $(\text{Dy,Yb})_2\text{Mn}_2\text{O}_7$  and the  $(\text{Dy,Lu})_2\text{Mn}_2\text{O}_7$  systems, which is consistent with the presence of an RSG-like magnetic state.<sup>17–19</sup> This is in accordance with the fact that be-

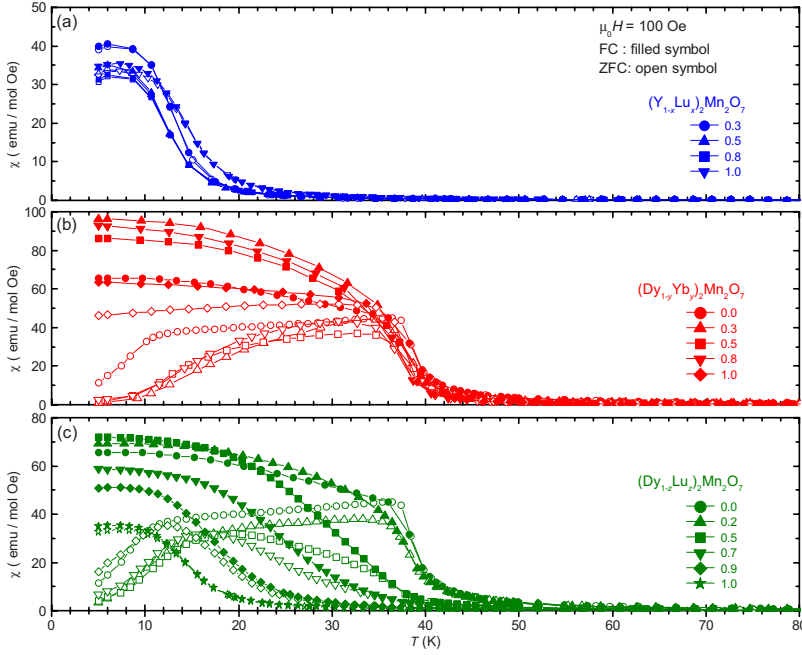


FIG. 2. (Color online) Temperature ( $T$ ) dependence of magnetic susceptibility ( $\chi$ ) for (a)  $(Y_{1-x}Lu_x)_2Mn_2O_7$ , (b)  $(Dy_{1-y}Yb_y)_2Mn_2O_7$ , and (c)  $(Dy_{1-z}Lu_z)_2Mn_2O_7$ , measured in both ZFC and FC modes under 100 Oe.

sides the magnetic  $Mn^{4+}$  ions, there are magnetic  $R^{3+}$  ions in the latter two systems such that additional  $R^{3+}-R^{3+}$  and/or  $R^{3+}-Mn^{4+}$  magnetic interactions may exist.

Magnetization ( $M$ ) data measured at 5 K with respect to applied magnetic field ( $H$ ) are shown in Figs. 4(a)–4(c). Nearly complete saturation is seen for all the samples; the slight but continuous rise of magnetization with increasing magnetic field infers the presence of an SG-like state since the orbital angular momentum on the  $Mn^{4+}$  ions is quenched.<sup>19</sup> For the  $(Y_{1-x}Lu_x)_2Mn_2O_7$  samples, the estimated magnetic moment *per*  $Mn^{4+}$  ion approaches but does not reach the theoretical value of  $3 \mu_B$ , see Fig. 4(a), con-

sistent with a frustrated AFM spin component of the Mn sublattice. As reported previously for  $R_2Mn_2O_7$  ( $R=Ho, Yb$ ) (Ref. 18) and also revealed in our earlier study on  $(Dy, Lu)_2Mn_2O_7$ ,<sup>19</sup> saturation of the Mn sublattice, which couples ferromagnetically with the R sublattice, does not depend significantly on the R composition. Hence we subtracted the magnetization curve of  $Lu_2Mn_2O_7$  from those for  $(Dy_{1-y}Yb_y)_2Mn_2O_7$  and  $(Dy_{1-z}Lu_z)_2Mn_2O_7$  in Figs. 4(b) and 4(c), respectively, in order to reveal the magnetization contribution purely from the magnetic rare-earth sublattice. Let us discuss the  $M-H$  curves for the  $(Dy_{1-y}Yb_y)_2Mn_2O_7$  system given in Fig. 4(b). The estimated saturation moment for the (Dy, Yb) sublattice at  $y=0.0$  (or the Dy sublattice) is close to that previously reported for  $(Dy, Y)_2Ti_2O_7$  (Ref. 25) and  $Dy_2Nb_2O_7$ .<sup>32</sup> Then with increasing Yb-for-Dy substitution level  $y$ , the saturation moment *per*  $R^{3+}$  cation gradually decreases such that at  $y=1.0$  ( $Yb_2Mn_2O_7$ ), the saturation magnetization for the Yb sublattice is close to the reported value for other Yb-based pyrochlore oxides.<sup>32–35</sup> We conclude that in high (5 T) magnetic fields, both the Mn and R sublattices are FM and approach saturation; the FM  $R^{3+}-Mn^{4+}$  spin-spin interactions suppress the frustrated-AFM component on the  $Mn^{4+}$ -ion array that is manifest at lower fields in  $(Y_{1-x}Lu_x)_2Mn_2O_7$ . However, at lowest temperatures,  $R^{3+}-R^{3+}$  interactions may introduce in zero magnetic field another magnetic frustration that is amplified by a crystalline anisotropy of the orientation of the rare-earth moment.

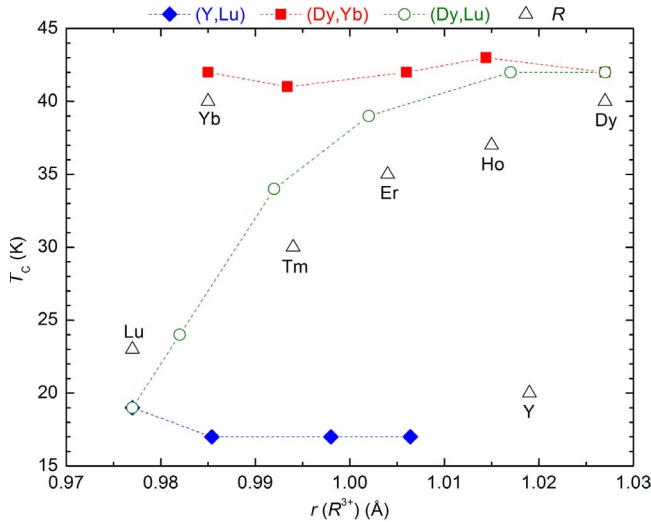


FIG. 3. (Color online)  $T_C$  versus  $r(R^{3+})$  (=average ionic radius of the R-site cations) for the present sample series of  $(Y_{1-x}Lu_x)_2Mn_2O_7$  ( $\blacklozenge$ ),  $(Dy_{1-y}Yb_y)_2Mn_2O_7$  ( $\blacksquare$ ), and  $(Dy_{1-z}Lu_z)_2Mn_2O_7$  ( $\circ$ ) and also in comparison for the  $R_2Mn_2O_7$  ( $\triangle$ ) phases (as given in Ref. 31). The value of  $T_C$  is estimated from the magnetic-susceptibility data.

#### IV. CONCLUSIONS

We synthesized and characterized three types of  $R_2Mn_2O_7$  pyrochlore rare-earth solid-solution systems, i.e., (i) nonmagnetic R  $(Y, Lu)_2Mn_2O_7$ , (ii) magnetic-moment-diluted  $(Dy, Yb)_2Mn_2O_7$ , and (iii) magnetic-ion-diluted  $(Dy, Lu)_2Mn_2O_7$ . The saturation magnetization of the  $(Y, Lu)_2Mn_2O_7$  system approaches, but does not reach by 5

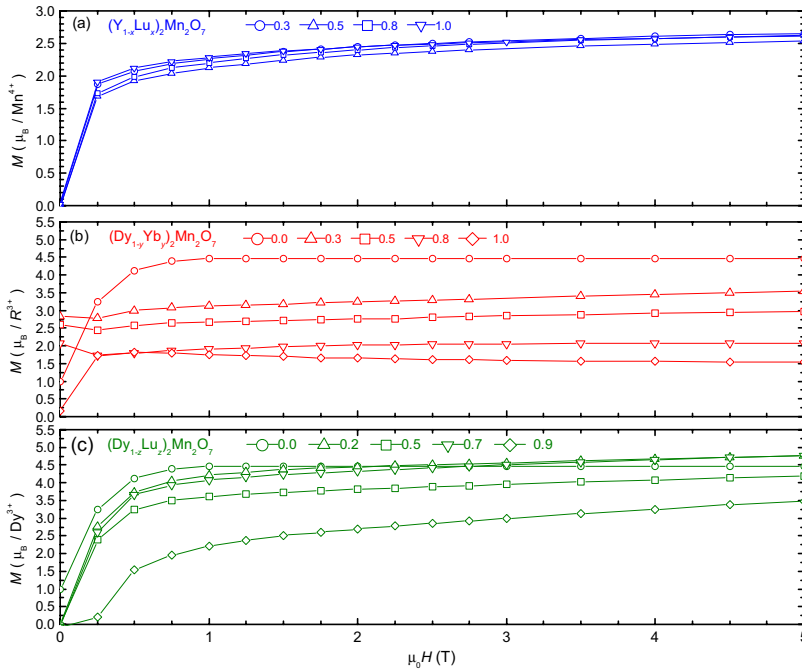


FIG. 4. (Color online) Magnetic field ( $H$ ) dependence of magnetization ( $M$ ) for (a)  $(Y_{1-x}Lu_x)_2Mn_2O_7$ , (b)  $(Dy_{1-y}Yb_y)_2Mn_2O_7$ , and (c)  $(Dy_{1-z}Lu_z)_2Mn_2O_7$ . The magnetization curves per  $R/Dy$  cation [(b) and (c)] were estimated by subtracting that of  $Lu_2Mn_2O_7$  (see the text in detail).

T, the  $3 \mu_B/Mn^{4+}$  that is attained with  $Tl_2Mn_2O_7$  and  $In_2Mn_2O_7$ , which indicates the presence of a minor, frustrated AFM component competing with the FM  $Mn^{4+}$ -O- $Mn^{4+}$  interactions in the  $(Y, Lu)_2Mn_2O_7$  system. In low applied magnetic fields at low temperatures, the AFM component of the interactions gives a magnetic susceptibility characteristic of an RSG like. The systems containing a spin on the  $R^{3+}$  ion exhibit a  $T_C$  that increases significantly with the concentration of the  $R^{3+}$  ions having a spin. This observation shows that FM  $R^{3+}$ - $Mn^{4+}$  interactions favor FM alignment of the  $Mn^{4+}$ -ion spins, thus reducing the net AFM frac-

tion of the interactions to relieve the frustration and raise  $T_C$  remarkably. The  $R^{3+}$ -ion size has little effect on the magnetic interactions; in the pyrochlore structure, the Mn-O-Mn bond angle varies little with  $R^{3+}$ -ion size.

#### ACKNOWLEDGMENTS

The present work was partially supported by Academy of Finland (Grant No. 126528) and Tekes (Grant No. 1726/31/07).

\*FAX: +358 9 462 373; maarit.karppinen@tkk.fi

<sup>1</sup>For review see J. S. Gardner, M. J. P. Gingras, and J. E. Greedan, *Rev. Mod. Phys.* **82**, 53 (2010).

<sup>2</sup>N. Hanasaki *et al.*, *Phys. Rev. Lett.* **99**, 086401 (2007).

<sup>3</sup>J. E. Greedan *et al.*, *Phys. Rev. B* **79**, 014427 (2009).

<sup>4</sup>A. P. Ramirez *et al.*, *Nature (London)* **399**, 333 (1999).

<sup>5</sup>J. Snyder *et al.*, *Nature (London)* **413**, 48 (2001).

<sup>6</sup>S. T. Bramwell and M. J. P. Gingras, *Science* **294**, 1495 (2001).

<sup>7</sup>M. J. P. Gingras *et al.*, *Phys. Rev. B* **62**, 6496 (2000).

<sup>8</sup>Y. Shimakawa, Y. Kudo, and T. Manako, *Nature (London)* **379**, 53 (1996).

<sup>9</sup>M. A. Subramanian *et al.*, *Science* **273**, 81 (1996).

<sup>10</sup>Y. Taguchi *et al.*, *Science* **291**, 2573 (2001).

<sup>11</sup>M. Hanawa *et al.*, *Phys. Rev. Lett.* **87**, 187001 (2001).

<sup>12</sup>M. A. Subramanian *et al.*, *J. Solid State Chem.* **72**, 24 (1988).

<sup>13</sup>J. E. Greedan, N. P. Raju, and M. A. Subramanian, *Solid State Commun.* **99**, 399 (1996).

<sup>14</sup>Y. Shimakawa *et al.*, *Phys. Rev. B* **59**, 1249 (1999).

<sup>15</sup>J. B. Goodenough, *Phys. Rev.* **100**, 564 (1955).

<sup>16</sup>J. Kanamori, *J. Phys. Chem. Solids* **10**, 87 (1959).

<sup>17</sup>J. N. Reimers *et al.*, *Phys. Rev. B* **43**, 3387 (1991).

<sup>18</sup>J. E. Greedan *et al.*, *Phys. Rev. B* **54**, 7189 (1996).

<sup>19</sup>N. Imamura, M. Karppinen, and H. Yamauchi, *Solid State Com-*

*mun.* **144**, 98 (2007).

<sup>20</sup>N. Ali *et al.*, *J. Solid State Chem.* **83**, 178 (1989).

<sup>21</sup>N. Taira, M. Wakeshima, and Y. Hinatsu, *J. Phys.: Condens. Matter* **11**, 6983 (1999).

<sup>22</sup>M. Ito *et al.*, *J. Phys. Chem. Solids* **62**, 337 (2001).

<sup>23</sup>N. Taira, M. Wakeshima, and Y. Hinatsu, *J. Mater. Chem.* **12**, 1475 (2002).

<sup>24</sup>B. Martínez *et al.*, *Phys. Rev. B* **46**, 10786 (1992).

<sup>25</sup>J. Snyder *et al.*, *Phys. Rev. B* **70**, 184431 (2004).

<sup>26</sup>M. Sato and J. E. Greedan, *J. Solid State Chem.* **67**, 248 (1987).

<sup>27</sup>T. Katsufuji, H. Y. Hwang, and S.-W. Cheong, *Phys. Rev. Lett.* **84**, 1998 (2000).

<sup>28</sup>Y. Moritomo *et al.*, *Phys. Rev. B* **63**, 144425 (2001).

<sup>29</sup>V. Prticek, M. Dusek, and L. Palatinus, Institute of Physics, Praha, Czech Republic, 2000.

<sup>30</sup>R. D. Shannon, *Acta Crystallogr., Sect. A: Cryst. Phys., Diffr., Theor. Gen. Crystallogr.* **32**, 751 (1976).

<sup>31</sup>M. A. Subramanian *et al.*, *J. Phys. IV* **07**, C1-625 (1997).

<sup>32</sup>O. Sakai *et al.*, *J. Phys. Soc. Jpn.* **73**, 2829 (2004).

<sup>33</sup>L. Soderholm, J. E. Greedan, and M. F. Collins, *J. Solid State Chem.* **35**, 385 (1980).

<sup>34</sup>S. T. Bramwell *et al.*, *J. Phys.: Condens. Matter* **12**, 483 (2000).

<sup>35</sup>J. A. Hodges *et al.*, *Phys. Rev. Lett.* **88**, 077204 (2002).